Palladium-Catalyzed Asymmetric Arylation of 2,3-Dihydrofuran with Phenyl Triflate. A Novel Asymmetric Catalysis Involving a Kinetic Resolution Process

Fumiyuki Ozawa,* Akihiko Kubo, Yonetatsu Matsumoto, and Tamio Hayashi*

Catalysis Research Center and Graduate School of Pharmaceutical Sciences, Hokkaido University, Kita-ku, Sapporo 060, Japan

Eriko Nishioka, Kazunori Yanagi,* and Koh-ichi Moriguchi

The Tsukuba Research Laboratory, Sumitomo Chemical Co., Ltd., Kitahara, Tsukuba 300-32, Japan

Received June 1, 1993⊗

The reaction of phenyl triflate and 2,3-dihydrofuran in benzene in the presence of a base and a palladium catalyst coordinated with (*R*)-BINAP gave optically active (*R*)-2-phenyl-2,3-dihydrofuran (**1a**) and a small amount of (*S*)-2-phenyl-2,5-dihydrofuran (**2a**). The two regioisomers have configurations opposite to each other. A clear correlation was observed between the enantioselectivity and the regioselectivity. Thus, the enantiomeric purity of (*R*)-**1a** increases as the ratio of (*S*)-**2a** to (*R*)-**1a** increases. A catalytic mechanism involving a kinetic resolution process is proposed to account for the relation. Factors controlling the regio- and enantioselectivities are discussed in detail using molecular models based on the X-ray structure of $PdCl_2$-{(*R*)-BINAP}. Crystal data for $PdCl_2$-{(*R*)-BINAP}: $C_{44}H_{32}Cl_2P_2Pd$, $a = 11.751(1)$ Å, $c = 26.538(3)$ Å, $V = 3664.2$ Å^3, tetragonal, $P4_1$, $Z = 4$.

Introduction

The palladium-catalyzed arylation and alkenylation of olefins (Heck reactions) are useful synthetic means of carbon–carbon bond formation.[1] These reactions have been extensively applied to organic synthesis during the past two decades. However, no reports on the "asymmetric Heck reaction" have appeared until very recently. In 1989, Shibasaki and Overman independently reported their pioneering works on the asymmetric Heck reaction, where intramolecular cyclization of alkenyl iodide or triflate forms chiral cyclic compounds of around 45% ee.[2,3] They improved the enantioselectivity and applied the reactions to asymmetric synthesis of *cis*-decalins (92% ee),[4] capnellenes (80% ee),[5] hydrindans (86% ee),[6] and spirooxindoles (95% ee).[7,8]

On the other hand, we reported the first example of an intermolecular asymmetric Heck reaction.[9,10] Treatment of 2,3-dihydrofuran with aryl triflates in benzene in the presence of a base and a palladium catalyst, generated in situ from $Pd(OAc)_2$ and (*R*)-BINAP,[11] gives (*R*)-2-aryl-2,3-dihydrofuran (**1**) and its regioisomer (*S*)-2-aryl-2,5-dihydrofuran (**2**) (eq 1).[12,13] The enantiomeric purity of the major product (*R*)-**1** exceeded 96% ee for a variety of aryl triflates under appropriate conditions.[9b]

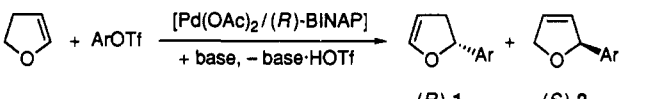

Ar = Ph, *p*-ClC_6H_4, *m*-ClC_6H_4, *o*-ClC_6H_4, *p*-AcC_6H_4, *p*-NCC_6H_4, *p*-$MeOC_6H_4$, 2-naphthyl

(*R*)-**1** (*S*)-**2** (1)

There are two points to note in the process of obtaining (*R*)-**1** of over 96% ee. The first is the use of aryl triflates as arylating reagents. Thus, the reaction using aryl iodide instead of aryl triflate gave racemic products. We reasoned that the high enantioselectivity observed with aryl triflates can be attributed to the reaction mechanism involving a cationic arylpalladium olefin intermediate.[9a] Scheme I

⊗ Abstract published in *Advance ACS Abstracts*, September 15, 1993.

(1) (a) Mizoroki, T.; Mori, K.; Ozaki, A. *Bull. Chem. Soc. Jpn.* **1971**, *44*, 581. (b) Mori, K.; Mizoroki, T.; Ozaki, A. *Bull. Chem. Soc. Jpn.* **1973**, *46*, 1505. (c) Heck, R. F.; Nolley, J. P., Jr. *J. Org. Chem.* **1972**, *37*, 2320. (d) Dieck, H. A.; Heck, R. F. *J. Am. Chem. Soc.* **1974**, *96*, 1133. (e) Heck, R. F. *Org. React.* **1982**, *27*, 345. (f) Heck, R. F. *Acc. Chem. Res.* **1979**, *12*, 146. (g) Heck, R. F. In *Palladium Reagents in Organic Synthesis*; Academic Press: New York, 1985. (h) Daves, G. D., Jr.; Hallberg, A. *Chem. Rev.* **1989**, *89*, 1433.

(2) Sato, Y.; Sodeoka, M.; Shibasaki, M. *J. Org. Chem.* **1989**, *54*, 4738.

(3) Carpenter, N. E.; Kucera, D. J.; Overman, L. E. *J. Org. Chem.* **1989**, *54*, 5846.

(4) Sato, Y.; Watanabe, S.; Shibasaki, M. *Tetrahedron Lett.* **1992**, *33*, 2589. Sato, Y.; Sodeoka, M.; Shibasaki, M. *Chem. Lett.* **1990**, 1953.

(5) Kagechika, K.; Shibasaki, M. *J. Org. Chem.* **1991**, *56*, 4093.

(6) Sato, Y.; Honda, T.; Shibasaki, M. *Tetrahedron Lett.* **1992**, *33*, 2593.

(7) Ashimori, A.; Overman, L. E. *J. Org. Chem.* **1992**, *57*, 4571.

(8) Other examples of the asymmetric Heck reaction: Brunner, H.; Kramler, K. *Synthesis* **1991**, 1121. Sakamoto, T.; Kondo, Y.; Yamanaka, H. *Tetrahedron Lett.* **1992**, *33*, 6845.

(9) Parts of these results have been reported in preliminary form: (a) Ozawa, F.; Kubo, A.; Hayashi, T. *J. Am. Chem. Soc.* **1991**, *113*, 1417. (b) Ozawa, F.; Kubo, A.; Hayashi, T. *Tetrahedron Lett.* **1992**, *33*, 1485.

(10) Ozawa, F.; Hayashi, T. *J. Organomet. Chem.* **1992**, *428*, 267. Ozawa, F.; Kobatake, Y.; Hayashi, T. *Tetrahedron Lett.* **1993**, *34*, 2505.

(11) (*R*)-BINAP = (*R*)-2,2′-bis(diphenylphosphino)-1,1′-binaphthyl. Takaya, T.; Mashima, K.; Koyano, K.; Yagim M.; Kumobayashi, H.; Taketomi, T.; Akutagawa, S.; Noyori, R. *J. Org. Chem.* **1986**, *51*, 629 and references cited therein.

(12) For Heck reactions of 2,3-dihydrofuran in nonasymmetric systems, see: Larock, R. C.; Gong, W. H. *J. Org. Chem.* **1990**, *55*, 407. Larock, R. C.; Gong, W. H.; Baker, B. E. *Tetrahedron Lett.* **1989**, *30*, 2603. Larock, R. C.; Baker, B. E. *Tetrahedron Lett.* **1988**, *29*, 905. Larock, R. C.; Gong, W. H. *J. Org. Chem.* **1989**, *54*, 2047.

(13) Note that, in this paper, the term "regioisomer" denotes the positional isomer of the C=C double bond of 2-phenyldihydrofurans (**1a** and **2a**), not the positional isomer of phenyl-substituted carbon, and the term "regioselectivity" describes the selectivity in forming **1a** or **2a**.

0276-7333/93/2312-4188$04.00/0

Scheme I. Proposed Mechanism for the Catalytic Arylation of 2,3-Dihydrofuran with Phenyl Triflate in the Presence of $Pd(OAc)_2$-(*R*)-BINAP Catalyst

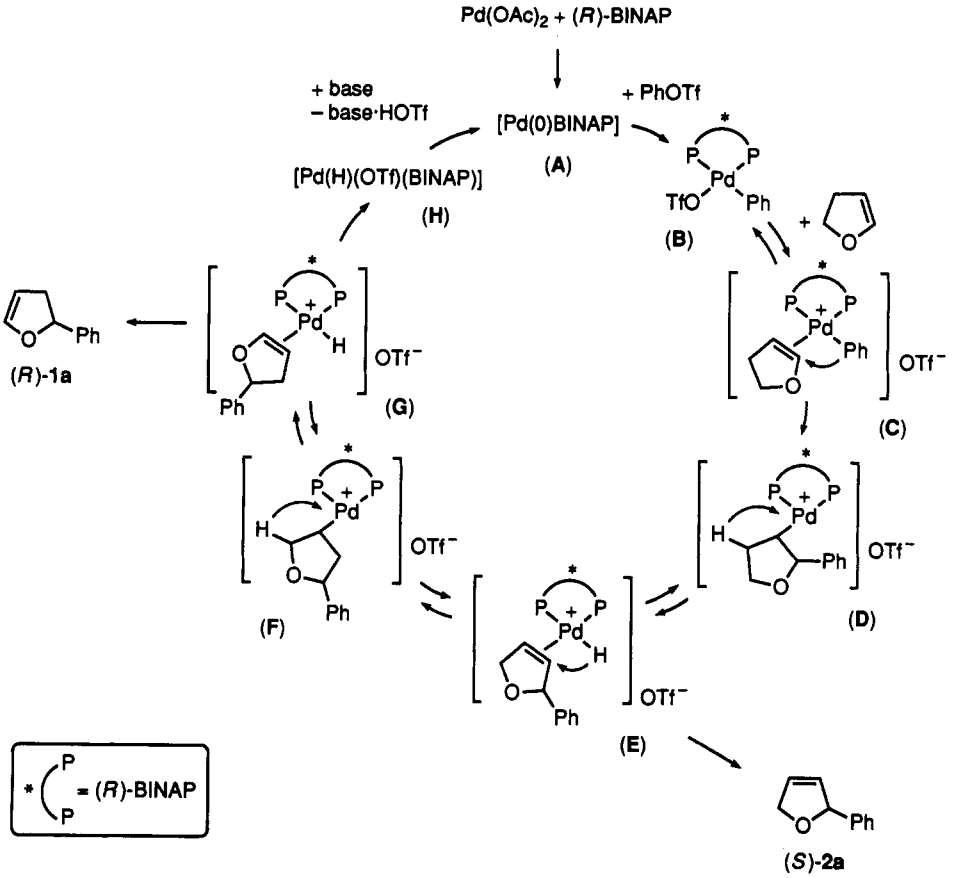

illustrates our proposed catalytic cycle for the phenylation reaction. Oxidative addition of phenyl triflate to a palladium(0)–BINAP species (**A**) gives a phenylpalladium triflate (**B**). Since the triflate ligand in **B** is a good leaving group, coordination of 2,3-dihydrofuran on **B** induces dissociation of the triflate ligand to give the cationic phenylpalladium olefin species (**C**), which has a 16-electron square-planar structure convenient for the subsequent enantioselective insertion of olefin.[14,15]

The second point is related to a unique process operative in the present asymmetric catalysis. Several lines of evidence indicated that the reaction involves a novel kinetic resolution process that efficiently enhances the enantiomeric purity of major product (*R*)-**1** by selective elimination of *S* isomer as the minor product **2** from the catalytic cycle.[16] In this paper we describe full details of our effort to clarify the kinetic resolution process. Acetate anion generated from $Pd(OAc)_2$ as the catalyst precursor was found to play a crucial role in the kinetic resolution.

Results

Catalytic Reaction. Base and catalyst precursor have prominent effects on the regio- and enantioselectivities. We examine both of these factors in the catalytic reaction of phenyl triflate and 2,3-dihydrofuran, giving (*R*)-2-phenyl-2,3-dihydrofuran (**1a**) and (*S*)-2-phenyl-2,5-dihydrofuran (**2a**).

Table I summarizes the effect of bases, showing that the basicity serves as the most important factor. The highest ratio of **2a** to **1a** was obtained in the presence of Proton Sponge (1,8-bis(dimethylamino)naphthalene) of the highest basicity ($pK_a = 12.34$)[17] (entry 1). In contrast, no formation of **2a** was observed in the presence of pyridine derivatives of the lowest basicity ($pK_a \approx 5$) (entries 6 and 7). Aliphatic amines ($pK_a \approx 11$) provided intermediate regioselectivities (entries 2–5).

It is interesting to note the relation between the product ratio and the enantiomeric purity of major product (*R*)-**1a**. Thus, the enantiomeric purity of (*R*)-**1a** tends to increase as the ratio of (*S*)-**2a** to (*R*)-**1a** increases. The highest enantiomeric purity of (*R*)-**1a** (>96% ee) was obtained in the reaction using Proton Sponge as the base, where the highest ratio of (*S*)-**2a** to (*R*)-**1a** was formed (entry 1). In contrast, the reactions using pyridine derivatives gave (*R*)-**1a** of much lower enantiomeric purities (67–77% ee) (entries 6 and 7). In these cases no formation of **2a** was observed. The tendency observed in Table I strongly suggests the kinetic resolution process.

A striking difference in the product ratio (**1a**:**2a**) was observed depending on the catalyst precursors (eqs 2 and

(14) Recently, we and another group independently showed that a cationic organopalladium complex having a structure closely related to **C** possesses extremely high reactivity toward olefin insertion: Ozawa, F.; Hayashi, T.; Koide, H.; Yamamoto, A. *J. Chem. Soc., Chem. Commun.* **1991** 1469. Dekker, G. P. C. M.; Elsevier, C. J.; Vrieze, K.; van Leeuwen, P. W. N. M. *J. Organomet. Chem.* **1992**, *430*, 357.

(15) A cationic arylpalladium intermediate has been independently proposed for the Heck reaction using aryl triflates: Cabri, W.; Candiani, I.; DeBernardinis, S.; Francalani, F.; Penco, S. *J. Org. Chem.* **1991**, *56*, 5796. Cabri, W.; Candiani, I.; Bedeschi, A.; Penco, S. *J. Org. Chem.* **1992**, *57*, 1481. Cabri, W.; Candiani, I.; Bedeschi, A.; Roberto, S. *J. Org. Chem.* **1992**, *57*, 3558.

(16) Examples of enantioselective catalysis involving a kinetic resolution process: Schreiber, S. L.; Schreiber, T. S.; Smith, D. B. *J. Am. Chem. Soc.* **1987**, *109*, 1525. Dokuzovic, Z. D.; Roberts, N. K.; Sawyer, J. F.; Whelan, J.; Bosnich, B. *J. Am. Chem. Soc.* **1986**, *108*, 2034.

(17) pK_a value of the conjugate acid: Alder, R. W.; Bowman, P. S.; Steele, W. R. P.; Winterman, D. R. *J. Chem. Soc., Chem. Commun.* **1968**, 723.

Table I. Effect of Organic Bases on the Catalytic Arylation of 2,3-Dihydrofuran with Phenyl Triflate[a]

entry no.	base	1a:2a[b]	% ee[c] (% yield)[d] (*R*)-1a	(*S*)-2a
1	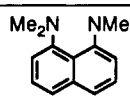	71:29	>96 (46)	17 (24)
2	Cy_2NH[e]	86:14	82 (59)	43 (4)
3	i-Pr_2NH	87:13	83 (73)	57 (9)
4	i-Pr_2NEt	92:8	82 (57)	60 (6)
5	Et_3N	98:2	75 (64)	9 (2)
6	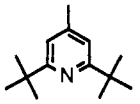	100:0	77 (23)	– (0)
7	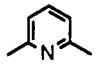	100:0	67 (27)	– (0)

[a] The reaction was carried out in benzene at 40 °C in the presence of $Pd(OAc)_2$ and (*R*)-BINAP (2 equiv/equiv of Pd) as the catalyst precursors. Initial conditions: $Pd(OAc)_2$:(*R*)-BINAP:PhOTf:2,3-dihydrofuran:base = 0.03:0.06:1:5:3. Reaction time (h): 216 (entries 1 and 7), 17 (entry 2), 72 (entry 3), 24 (entry 4), 26 (entry 5), 120 (entry 6). Conversion of PhOTf (%): 100 (entries 1–5), 88 (entry 6), 38 (entry 7). [b] The product ratio in the reaction solution as determined by GLC. [c] Determined by ^1H NMR using $Eu(hfc)_3$. [d] Isolated yield. [e] Cy_2NH = dicyclohexylamine.

3). The reaction using $Pd(OAc)_2$ and (*R*)-BINAP as

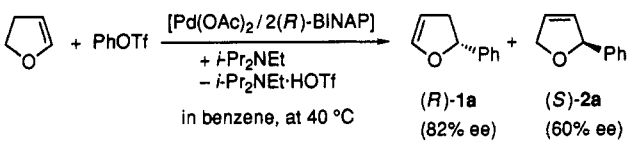

(2)

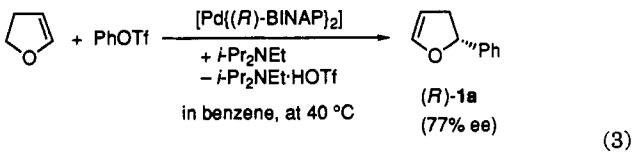

(3)

catalyst precursors gave (*R*)-**1a** and (*S*)-**2a** in a 92:8 ratio (eq 2). In contrast, no formation of **2a** was observed in the reaction using isolated $Pd\{(R)\text{-BINAP}\}_2$ catalyst (eq 3). The enantiomeric purity of (*R*)-**1a** was higher in eq 2 than in eq 3.

It is generally accepted that $Pd(OAc)_2$ employed in the Heck reaction is reduced to a catalytically active palladium(0) species.[1e] We recently confirmed that the reduction giving the BINAP-coordinated palladium(0) species proceeds according to eq 4, where 1 equiv of BINAP monoxide and 2 equiv of ammonium acetate are formed.[18]

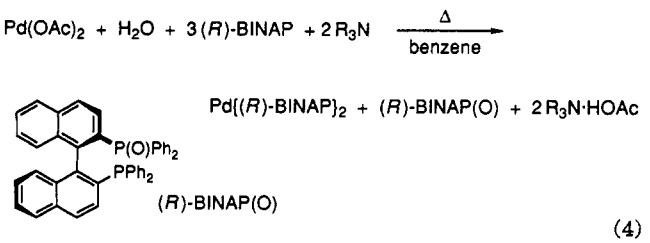

(4)

Therefore, we examine the effects of these products on the catalytic reaction using $Pd\{(R)\text{-BINAP}\}_2$ (Table II). BINAP monoxide had no effect on the catalytic system (entry 2). In contrast, addition of acetic acid, which forms ammonium acetate in the system containing an excess amount of amine, caused the formation of (*S*)-**2a** (entries 3–5). The larger amount of acetic acid gave rise to the higher ratio of (*S*)-**2a** to (*R*)-**1a**. The enantiomeric purity of (*R*)-**1a** increased as the amount of acetic acid increased until 5 equiv of acetic acid/equiv of Pd was added (entries 3 and 4). Further addition of acetic acid (10 equiv/equiv of Pd) resulted in a significant drop in the enantiomeric purity despite the increase in the ratio of (*S*)-**2a** to (*R*)-**1a** (entry 5).

Table II. Effect of Additives on the Catalytic Asymmetric Arylation of 2,3-Dihydrofuran with Phenyl Triflate in the Presence of $Pd\{(R)\text{-BINAP}\}_2$ Catalyst[a]

entry no.	additive (amt, (equiv/equiv of Pd))	1a:2a[b]	% ee[c] (% yield)[d] (*R*)-1a	(*S*)-2a
1		100:0	77 (59)	
2	(*R*)-BINAP(O) (1)	100:0	76 (62)	
3	AcOH (2)	89:11	83 (58)	64 (8)
4	AcOH (5)	84:16	>96 (58)	60 (12)
5[e]	AcOH (10)	80:20	87 (50)	60 (5)
6	TsOH (5)	100:0	74 (63)	
7	CF_3CO_2H (5)	90:10	81 (63)	67 (7)
8	Me_2CHCO_2H (5)	85:15	96 (57)	60 (15)
9	$Me(CH_2)_2CO_2H$ (5)	76:24	86 (64)	67 (11)

[a] The reaction was carried out in benzene in the presence of i-Pr_2NEt as the base at 40 °C. Initial conditions: $Pd\{(R)\text{-BINAP}\}_2$:PhOTf:2,3-dihydrofuran:i-Pr_2NEt = 0.03:1:5:3. Reaction time (h): 28 (entry 7), 48 (entries 1–4 and 6), 96 (entries 5 and 9), 246 (entry 8). [b] The product ratio in the reaction solution as determined by GLC. [c] Determined by ^1H NMR using $Eu(hfc)_3$. [d] Isolated yield. [e] 40% of PhOTf was recovered unreacted.

Table III. Selected Bond Distances (Å) and Angles (deg) For $PdCl_2\{(R)\text{BINAP}\}$

Bond Distances			
Pd–Cl(1)	2.349(3)	P(2)–C(11)	1.835(9)
Pd–Cl(2)	2.349(3)	P(2)–C(33)	1.815(9)
Pd–P(1)	2.241(2)	P(2)–C(39)	1.84(1)
Pd–P(2)	2.248(2)	C(1)–C(10)	1.38(1)
P(1)–C(1)	1.843(9)	C(10)–C(20)	1.48(1)
P(1)–C(21)	1.820(9)	C(11)–C(20)	1.41(1)
P(1)–C(27)	1.81(1)		
Bond Angles			
CL(1)–P–P(1)	159.4(1)	Pd–P(2)–C(11)	110.5(3)
Cl(1)–Pd–P(2)	90.8(1)	Pd–P(2)–C(33)	118.6(3)
Cl(2)–Pd–P(1)	90.3(1)	Pd–P(2)–C(39)	109.8(4)
Cl(2)–Pd–P(2)	159.7(1)	C(11)–P(2)–C(33)	107.0(4)
P(1)–Pd–P(2)	92.69(8)	C(11)–P(2)–C(39)	102.9(4)
Pd–P(1)–C(1)	111.6(3)	C(33)–P(2)–C(39)	106.8(5)
Pd–P(1)–C(21)	118.4(3)	P(1)–C(1)–C(10)	121.4(7)
Pd–P(1)–C(27)	108.4(4)	C(1)–C(10)–C(20)	121.8(8)
C(1)–P(1)–C(21)	105.7(4)	C(10)–C(20)–C(11)	122.1(7)
C(1)–P(1)–C(27)	105.1(4)	P(2)–C(11)–C(20)	120.0(6)
C(21)–P(1)–C(27)	106.7(5)		

X-ray Structure of $PdCl_2\{(R)\text{-BINAP}\}$. In order to gain structural information on palladium species coordinated with the (*R*)-BINAP ligand, the crystal structure of $PdCl_2\{(R)\text{-BINAP}\}$ was examined by X-ray diffraction. Selected bond lengths and angles are listed in Table III. As can be seen from the ORTEP diagrams in Figure 1, the seven-membered heterometallacyclic ring formed by the

(18) Ozawa, F.; Kubo, A.; Hayashi, T. *Chem. Lett.* **1992**, 2177. A similar result has been reported: Amatore, C.; Jutand, A.; M'Barki, M. A. *Organometallics* **1992**, *11*, 3009. Mandai, T.; Matsumoto, T.; Tsuji, J. *Tetrahedron Lett.* **1993**, *34*, 2513. Grushin, V. V.; Alper, H. *Organometallics* **1993**, *12*, 1890.

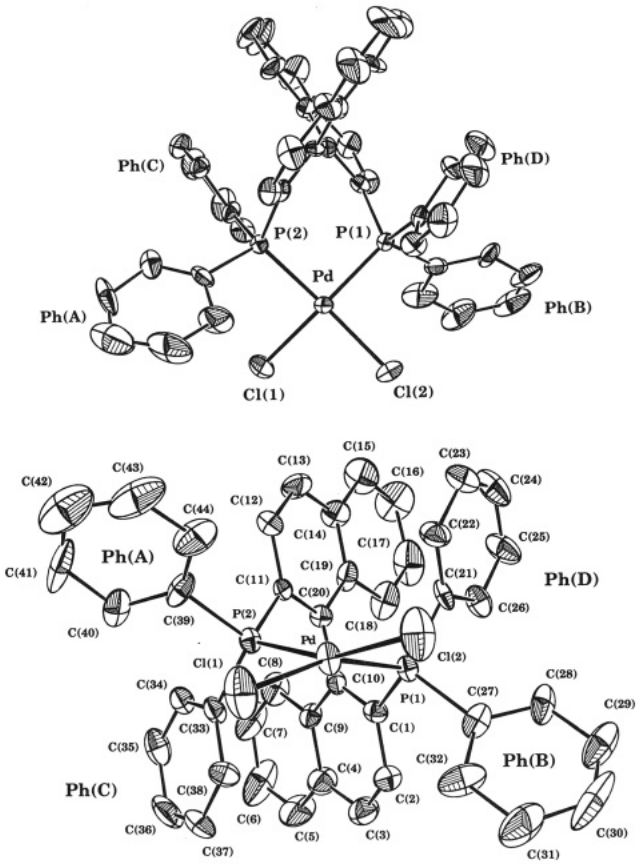

Figure 1. ORTEP diagrams of $PdCl_2\{(R)$-BINAP$\}$. The ellipsoids are drawn at the 30% probability level.

chelate coordination of the BINAP ligand is highly skewed. Two of the phenyl groups (Ph(C) and Ph(D)) are oriented axially and the other two phenyl groups (Ph(A) and Ph(B)) equatorially with respect to the P(1)–Pd–P(2) plane. The axial phenyl groups are accommodated at the sides of the binaphthyl group with apparent π–π stacking interactions with the naphthyl rings. On the other hand, the equatorial phenyl groups extrude toward the coordination sites of the chloride ligands. These structural features, commonly observed in BINAP-coordinated transition-metal complexes,[19] are attributed to the rigid nature of the backbone of the BINAP ligand. It can be seen that considerable steric hindrance exists between the equatorial phenyl groups and the chloride ligands. The Cl(1) and Cl(2) atoms are situated below and above the P(1)–Pd–P(2) plane, respectively, to avoid the steric interaction with the equatorial phenyl groups. The complex has a distorted-square-planar structure, the sum of four angles at Pd involving Cl(1), Cl(2), P(1), and P(2) being 367.3(2)° and the bond angles of P(1)–Pd–Cl(1) and P(2)–Pd–Cl(2) being 159.4(1) and 159.7(1)°, respectively. The bite angle of the BINAP ligand (92.69(8)°) is among the largest values for BINAP-coordinated transition-metal complexes.[19] The Pd–P distances (2.241(2) and 2.248(2) Å) and the Pd–Cl distances (2.349(4) and 2.350(3) Å) are in the typical range for dichloropalladium complexes bearing diphosphine ligands.[20]

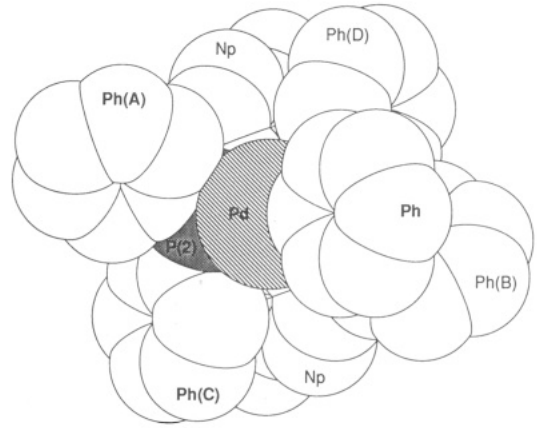

Figure 2. Molecular model of the $[PdPh\{(R)$-BINAP$\}]^+$ moiety. The structural parameters of the $[Pd\{(R)$-BINAP$\}]$ moiety is taken from the X-ray structure of $PdCl_2\{(R)$-BINAP$\}$. The Pd–Ph group is located on the P(1)–Pd–P(2) plane at the position cis to P(1) with a Pd–Ph bond length of 2.1 Å and a P(1)–Pd–Ph angle of 90°.

Discussion

One of the most interesting features in the present asymmetric reaction is the relation between the enantiomeric purity of major product (*R*)-**1a** and the regioselectivity of the reaction. Thus, a higher ratio of minor product (*S*)-**2a** to major isomer (*R*)-**1a** tends to provide a higher enantiomeric purity of (*R*)-**1a**. We first discuss the detailed mechanism of the reaction and then reason about the relationship.

The two regioisomers have absolute configurations opposite to each other. This fact indicates a catalytic process that selectively converts *R* and *S* phenylation products into **1a** and **2a**, respectively. In the present reaction using a chiral catalyst, the catalytic course in Scheme I branches into two routes at the stage of olefin coordination to **B**, depending on the selection of enantiofaces of 2,3-dihydrofuran. Figure 2 depicts a molecular view of the $[PdPh\{(R)$-BINAP$\}]^+$ moiety of the cationic phenylpalladium olefin intermediate (**C**), which was drawn with the partial X-ray structure of $PdCl_2\{(R)$-BINAP$\}$. It is seen that the lower part of the empty coordination site opens widely, whereas the upper part is blocked by one of the phenyl groups of the BINAP ligand (Ph(A)). Scheme II shows the two possible modes for the coordination of 2,3-dihydrofuran to the $[PdPh\{(R)$-BINAP$\}]^+$ moiety. In mode a dihydrofuran combines with the palladium center through the *si* face and in mode b through the *re* face. The olefin coordination in mode a followed by olefin-insertion and β-hydrogen-elimination reactions forms the phenylation product with *R* configuration. In contrast, the olefin coordination in mode b leads to the *S* phenylation product. As suggested from the molecular structure in Figure 2, mode a is apparently preferable to mode b, a significant steric repulsion between the equatorial phenyl group (Ph(A)) and dihydrofuran being observed in the latter case. Hence, the *R* isomer is the major product in the catalytic reactions.

(19) $[Rh(NBD\{(R)$-BINAP$\}]ClO_4$: Toriumi, K.; Ito, T.; Takaya, H.; Souchi, T.; Noyori, R. *Acta Crystallogr.* **1982**, *B38*, 807. $[Rh\{(R)$-BINAP$\}_2]ClO_4$: Tani, K.; Yamagata, T.; Tatsuno, Y.; Yamagata, Y.; Tomita, K.; Akutagawa, S.; Kumobayashi, H.; Otsuka, S. *Angew. Chem. Int. Ed. Engl.* **1985**, *24*, 217. $RuHCl\{(R)$-BINAP$\}_2$: Kawano, H.; Ishii, Y.; Kodama, T.; Saburi, M.; Uchida, Y. *Chem. Lett.* **1987**, 1311. $Ru(O_2CCMe_3)_2\{(S)$-BINAP$\}$: Ohta, T.; Takaya, H.; Noyori, R. *Inorg. Chem.* **1988**, *27*, 566. $[\{Rh((R)$-BINAP$)\}_3(\mu_3$-OD$)_2]ClO_4$: Yamagata, T.; Tani, K.; Tatsuno, Y.; Saito, T. *J. Chem. Soc., Chem. Commun.* **1988**, 466. $[RuCl(\eta^6$-$C_6H_6)\{(S)$-BINAP$\}]BF_4$: Mashima, K.; Kusano, K.; Ohta, T.; Noyori, R.; Takaya, H. *J. Chem. Soc., Chem. Commun.* **1989**, 1208. $[Ru\{(R)$-BINAP$\}(O_2CCMe{=}CHMe)_2]$: Ashby, M. T.; Khan, M. A.; Halpern, J. *Organometallics* **1991**, *10*, 2011.

(20) Steffen, W. L.; Palenik, G. J. *Inorg. Chem.* **1976**, *15*, 2432. Hayashi, T.; Konishi, M.; Kobori, Y.; Kumada, M.; Higuchi, T.; Hirotsu, K. *J. Am. Chem. Soc.* **1984**, 106, 158.

Scheme II. Schematic Process for the Enantioselective Insertion of 2,3-Dihydrofuran, Showing the Two Possible Modes (a) and (b) for Olefin Coordination[a]

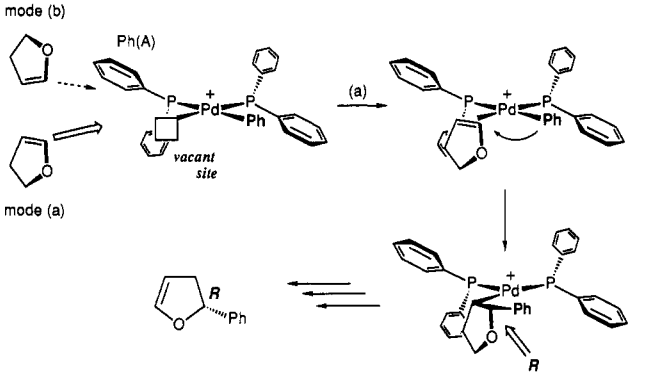

[a] The binaphthylene group in the (*R*)-BINAP ligand is omitted for clarity.

The formation of (*R*)-**1a** and (*S*)-**2a** can be rationalized by the mechanism illustrated in Scheme III, which comprises two reaction courses (*R* and *S* routes). Coordination of dihydrofuran in mode a and mode b forms the olefin-coordinated complexes $\mathbf{C}_R$ and $\mathbf{C}_S$, respectively. These complexes undergo olefin insertion into the Pd–Ph bond. The subsequent β-hydrogen elimination gives a pair of diasteromers of hydrido–olefin complexes bearing (*R*)- and (*S*)-2-phenyl-2,5-dihydrofuran ligands, $\mathbf{E}_R$ and $\mathbf{E}_S$, respectively. The experimental results indicate that $\mathbf{E}_S$ in the *S* route is prone to release the coordinated olefin (*S*)-**2a**, whereas $\mathbf{E}_R$ in the *R* route undergoes further olefin-insertion and β-hydrogen-elimination reactions to give a hydridopalladium species coordinated with (*R*)-2-phenyl-2,3-dihydrofuran ($\mathbf{G}_R$), which forms (*R*)-**1a**.

The difference in the reactivity between $\mathbf{E}_R$ and $\mathbf{E}_S$ can be understood using molecular models of these diastereomers (Scheme IV). As shown in Scheme II, insertion of the olefin in mode a gives alkyl complex $\mathbf{D}_R$. In the subsequent β-hydrogen elimination, the β-hydrogen bound to the C4 carbon of the tetrahydrofuran ring is abstracted by the palladium center. Since the β-hydrogen elimination requires an agostic interaction between the β-hydrogen and the palladium center,[21] the tetrahydrofuran ring must rotate around the Pd–C3 bond to allow the direct interaction of the β-hydrogen with the vacant site at the palladium center. Accordingly, the hydrido–olefin complex resulting from the β-hydrogen elimination has the structure of $\mathbf{E}_R$-1, which suffers considerable steric repulsion between the coordinated olefin and the equatorial phenyl group of the BINAP ligand. The steric repulsion is effectively released by rotation of the olefin ligand around the Pd–olefin bond, giving $\mathbf{E}_R$-**2**. This complex has a convenient structure for the formation of (*R*)-**1a**. Thus, migration of the hydrido ligand to the C3 carbon of the 2-phenyl-2,5-dihydrofuran ligand gives alkyl species $\mathbf{F}_R$. The subsequent β-hydrogen elimination from the C5 carbon adjacent to oxygen forms (*R*)-**1a**. Therefore, the formation of **1a** in the *R* route seems to proceed smoothly.

On the other hand, steric conditions in the *S* route make a similar sequence of reactions giving (*S*)-**1a** unfavorable. When 2,3-dihydrofuran undergoes the olefin insertion in mode b (Scheme II), the resulting alkyl species has the structure of $\mathbf{D}_S$ in Scheme IV. β-Hydrogen elimination from the C4 carbon of the tetrahydrofuran ring in $\mathbf{D}_S$ forms $\mathbf{E}_S$-1, where the 2-phenyl-2,5-dihydrofuran ligand is accommodated in the less sterically hindered site. For the formation of (*S*)-**1a**, $\mathbf{E}_S$-1 must be converted into $\mathbf{E}_S$-**2**. The fact that $\mathbf{E}_S$-**2** is more sterically congested than $\mathbf{E}_S$-1 makes the equilibrium between $\mathbf{E}_S$-1 and $\mathbf{E}_S$-**2** lie to the side of $\mathbf{E}_S$-1 and retards the formation of (*S*)-**1a**.

We have demonstrated that the present asymmetric catalysis involves an interesting process that selectively converts *R* and *S* phenylation products into **1a** and **2a**, respectively. This process provides (*R*)-**1a** of extremely high enantiomeric purity. Table IV shows the product distribution in the catalytic reactions listed in Table I. The *R*:*S* indicates the selectivity of enantiofaces of 2,3-dihydrofuran, namely the ratio of the *R* route to the *S* route. The table also includes the regioselectivity in each route. These values were calculated from the ratio of (*R*)-**1a** to (*S*)-**2a** and the enantiomeric purities of both products. The following points emerge from the data. (i) There is no correlation between the enantiomeric purity of (*R*)-**1a** and the selectivity of enantiofaces. (ii) The regioselectivity in the *S* route markedly varies with bases, but the variation in the regioselectivity in the *R* route is relatively small. (iii) The enantiomeric purity of (*R*)-**1a** remarkably increases as the selectivity of **2a** in the *S* route increases. These observations clearly indicate that the regioselectivity in the *S* route is the chief determining factor of the enantiomeric purity of (*R*)-**1a**.

The enantiomeric purity of (*R*)-**1a** is determined at two stages. At the first stage, the selection of enantiofaces of 2,3-dihydrofuran takes place. The ratio of the *R* route to the *S* route in Scheme III is determined at this stage. When both routes give only **1a**, the resulting product ((*R*)-**1a**) has an enantiomeric purity exactly reflecting the selectivity of enantiofaces. Such reactions proceed in the absence of acetate (eq 3) and in the presence of less basic pyridine derivatives (Table I, entries 6 and 7). On the other hand, when the *S* route forms **2a**, the enantiomeric purity of (*R*)-**1a** becomes higher than that expected from the selectivity of enantiofaces because the contamination of **1a** with the *S* isomer is prevented (Table IV, entries 1–5). The formation of (*S*)-**2a** takes place in the presence of acetate and basic amine.

The reason the formation of (*S*)-**2a** requires the presence of acetate anion can be explained as follows. Since the hydrido–olefin complex $\mathbf{E}_S$ has a 16-electron square-planar structure, dissociation of the coordinated olefin should proceed via an associative mechanism involving an 18-electron transition state formed by nucleophilic attack of an incoming ligand at the palladium center. The acetate anion may possess enough nucleophilicity toward the cationic palladium center in $\mathbf{E}_S$ to cause the dissociation of the olefin.

The nucleophilicity of acetate anion should be defined by the countercation, particularly in nonpolar media such as benzene. The marked difference in effect of bases on the regioselectivity in the *S* route is attributable to the difference in the nucleophilicity of acetate anion that is controlled by the ammonium cation. Proton Sponge, being one of the strongest bases for trapping proton in organic solvents, may generate the highly reactive acetate anion that efficiently induces the dissociation of (*S*)-**2a** from $\mathbf{E}_S$, resulting in the formation of almost enantiomerically pure (*R*)-**1a**.

Experimental Section

General Considerations. All manipulations were carried out under a nitrogen atmosphere using conventional Schlenk tech-

(21) Koga, N.; Morokuma, K. *Chem. Rev.* **1991**, *91*, 823.

Scheme III. Proposed Mechanisms for Stereoselective Formation of (*R*)-1a and (*S*)-2a

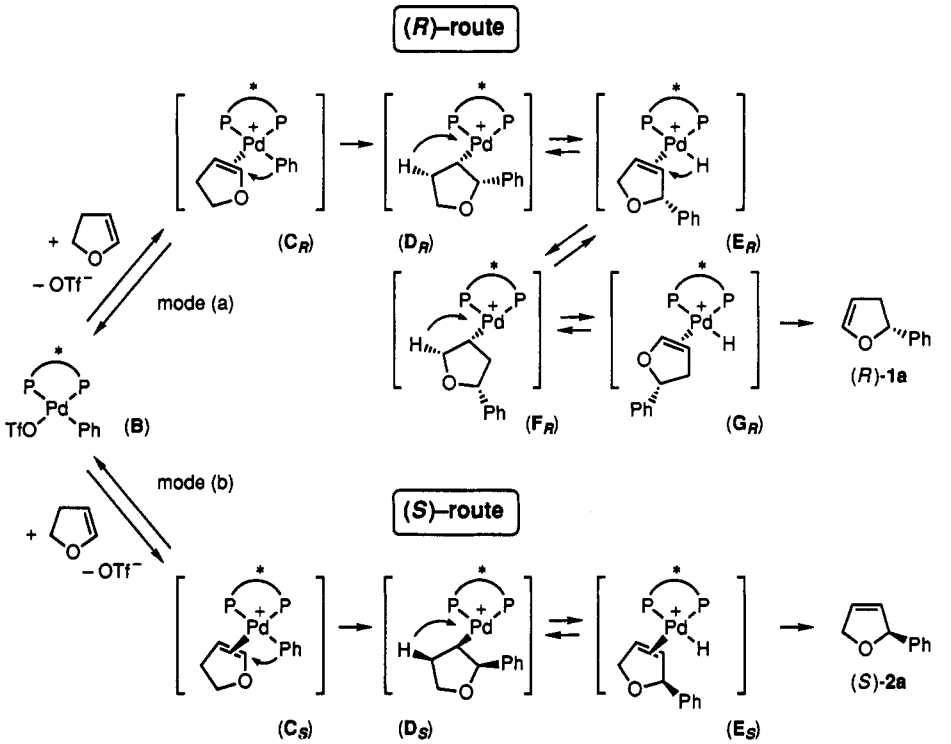

Scheme IV. Schematic Diagrams for Formation of (*R*)-1a and (*S*)-2a[a]

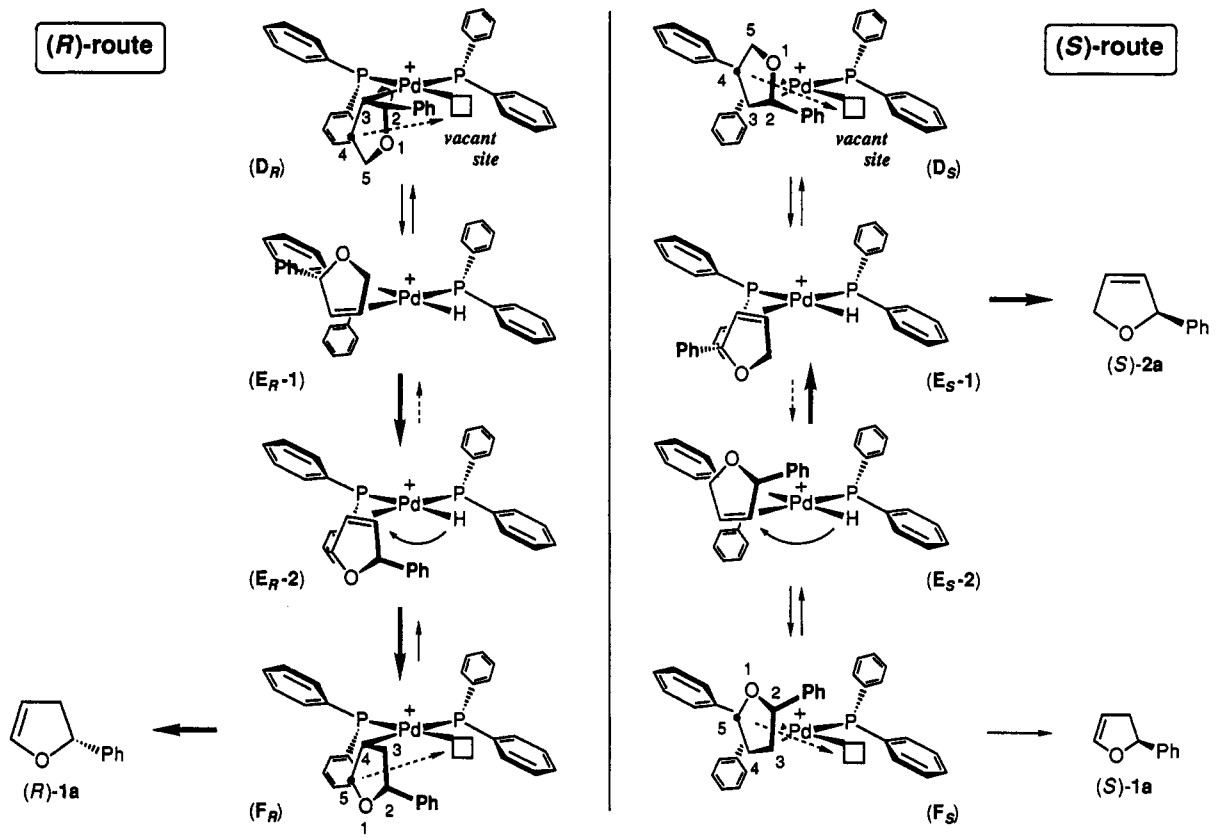

[a] The binaphthylene group in the (*R*)-BINAP ligand is omitted for clarity.

niques. Nitrogen gas was dried by passage through P_2O_5 (Merck, SICAPENT). NMR spectra were recorded on a JEOL JNM-EX90 spectrometer (^{1}H, 89.45 MHz; ^{31}P NMR, 36.10 MHz). Chemical shifts are reported in δ (ppm) referenced to an internal $SiMe_4$ standard for ^{1}H NMR and to an external 85% H_3PO_4 standard for ^{31}P NMR. IR spectra were recorded on a Perkin-Elmer 1720X FT-IR spectrometer. Optical rotations were measured on a JASCO DIP-370 polarimeter. Mass spectra (EI, 70 eV) were measured on a JEOL JMS-DX-303 spectrometer. Elemental analyses were performed by the Hokkaido University Analytical Center. Preparative medium-pressure liquid chromatography (MPLC) was performed with a prepacked silica gel column (Kusano CIG Si-10, 22 mm i.d. × 300 length). GLC analysis was carried out on a Shimadzu GC-7AG instrument, equipped with a FID detector and a 1-m glass column (3 mm i.d.) of 5% Silicone OV-1 on Chromosorb WAW DMCS.

Materials. Phenyl triflate was prepared by the reported method.[22] Amines were obtained from commercial sources and

Table IV. Product Distribution in the Asymmetric Heck Reaction Using Various Organic Bases

entry no.	base	enantioface selectivity[a]		regioselectivity,[a] 1a:2a		% ee of product (*R*)-1a
		R:*S*	*R* − *S*	*R* route	*S* route	
1	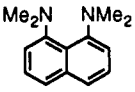	>82:18	>64	>85:15	<8:92	>96
2	Cy_2NH	82.5:17.5	65	95:5	44:56	82
3	*i*-Pr_2NH	82.5:17.5	65	97:3	42:58	83
4	*i*-Pr_2NEt	85:15	70	98:2	56:44	82
5	Et_3N	86.5:13.5	73	99:1	92:8	75
6	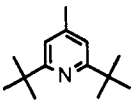	88.5:11.5	77	100:0	100:0	77
7		83.5:16.5	67	100:0	100:0	67

[a] The values were calculated from the data in Table I.

used without further purification. Palladium diacetate was purchased from Johnson Mathey and purified by recrystallization from hot benzene before use. (*R*)-(+)-2,2′-Bis(diphenylphosphino)-1,1′-binaphthyl ((*R*)-BINAP) was obtained from Kanto Chemical and used without further purification. Benzene and Et_2O were dried over sodium–benzophenone ketyl and distilled just before use. 1,2-Dichloroethane was dried over CaH_2, distilled, and stored under a nitrogen atmosphere.

Catalytic Reaction of 2,3-Dihydrofuran with Phenyl Triflate. A typical procedure (Table I, entry 4) is as follows. A mixture of $Pd(OAc)_2$ (8.7 mg, 0.039 mmol) and (*R*)-BINAP (49.3 mg, 0.079 mmol) in benzene (2 mL) was stirred under N_2 at room temperature for 10 min, and phenyl triflate (267 mg, 1.18 mmol) was added. Diisopropylethylamine (680 μL, 4.0 mmol) and 2,3-dihydrofuran (500 μL, 6.6 mmol) were added, and the homogeneous mixture was stirred at 40 °C for 24 h. GLC analysis of the dark red reaction mixture showed formation of 2-phenyl-2,3-dihydrofuran (**1a**) and 2-phenyl-2,5-dihydrofuran (**2a**) in a 92:8 ratio at 100% conversion of phenyl triflate. The mixture was poured into vigorously stirred pentane (ca. 300 mL), and the resulting red solid was removed by filtration. The filtrate was concentrated to dryness to give a pale red, oily material, which was subjected to MPLC (silica gel, 10/1 hexane/EtOAc) to give 97.6 mg (57% yield) of (*R*)-**1a** and 9.5 mg (5.5% yield) of (*S*)-**2a**. The enantiomeric purities of (*R*)-**1a** (82% ee) and (*S*)-**2a** (60% ee) were determined by ^1H NMR ($CDCl_3$) using the optically active NMR shift reagent tris[3-((heptafluoropropyl)hydroxymethylene)camphorato]europium(III) (Eu(hfc)$_3$). In the NMR analysis, the olefinic protons of (*R*)-**1a** appeared at higher field than those of (*S*)-**1a**, whereas the ortho protons of the phenyl group in (*S*)-**2a** appeared at lower field than those of (*R*)-**2a**.

All catalytic reactions reported in this paper were performed similarly, except for the reaction with Proton Sponge (Table I, entry 1). The reaction using Proton Sponge required treatment of the catalyst precursor (i.e. $Pd(OAc)_2$ and (*R*)-BINAP) with base prior to the catalytic reaction. In a Schlenk tube were placed $Pd(OAc)_2$ (13.4 mg, 0.060 mmol), (*R*)-BINAP (73.6 mg, 0.12 mmol), and 1.8-bis(dimethylamino)naphthalene (1.27 g, 5.9 mmol). The system was purged with nitrogen gas, and benzene (6 mL) was added. The pale yellow mixture was stirred at 40 °C for 2 h to give a red homogeneous solution. Phenyl triflate (424 mg, 1.87 mmol) and 2,3-dihydrofuran (770 μL, 10.2 mmol) were added, and the homogeneous solution was stirred at 40 °C for 9 days. GLC analysis showed the formation of **1a** and **2a** in a 71:29 ratio and complete consumption of phenyl triflate. The mixture was subjected directly to column chromatography (silica gel, CH_2Cl_2) to remove the ammonium salt and Proton Sponge. The eluate was concentrated to dryness to give a red oily material, which was further purified by MPLC (silica gel, 10/1 hexane/AcOEt) to give 125 mg (46% yield, >96% ee) of (*R*)-**1a** and 64 mg (24% yield, 17% ee) of (*S*)-**2a**.

(22) Stang, P. J.; Hanack, H.; Subramanian, L. R. *Synthesis* **1982**, 85.

(*R*)-(−)-2-Phenyl-2,3-dihydrofuran (1a, 93% ee): $[\alpha]_D^{20}$ = 64.3° (*c* = 1.2, $CHCl_3$); ^1H NMR ($CDCl_3$) δ 2.59 (ddt, *J* = 15.2, 8.4, 2.5 Hz, 1 H), 3.08 (ddt, *J* = 15.2, 10.6, 2.5 Hz, 1 H), 4.95 (q, *J* = 2.5 Hz, 1 H), 5.51 (dd, *J* = 10.6, 8.4 Hz, 1 H), 6.44 (q, *J* = 2.5 Hz, 1 H), 7.34 (m, 5 H); IR (KBr) 1620, 1136, 1052 cm^{-1}; HRMS (EI) calcd for $C_{10}H_{10}O$ 146.0731, found 146.0736. Anal. Calcd for $C_{10}H_{10}O$: C, 82.16; H, 6.89. Found: C, 82.08; H, 6.96.

(*S*)-(−)-2-Phenyl-2,5-dihydrofuran (2a, 67% ee): $[\alpha]_D^{20}$ = −175° (*c* = 1.3, $CHCl_3$); ^1H NMR ($CDCl_3$) δ 4.86 (m, 2 H), 5.76 (m, 1 H), 5.89 (dq, *J* = 5.9, 1.1 Hz, 1 H), 6.04 (dq, *J* = 5.9, 1.6 Hz, 1 H), 7.32 (m, 5 H); IR (KBr) 1620, 1081, 1064 cm^{-1}; HRMS (EI) calcd for $C_{10}H_{10}O$ 146.0731, found 146.0704. Anal. Calcd for $C_{10}H_{10}O$: C, 82.16; H, 6.89. Found: C, 82.12; H, 6.92.

Determination of Absolute Configuration of (*R*)-(−)-1a. The absolute configuration of (−)-**1a** was determined by converting it into known γ-butyrolactone derivative (*R*)-3-phenyl-2-oxacyclopentanone. (−)-**2a** (149.6 mg, 1.02 mmol, 84% ee) was placed in a Schlenk tube and dissolved in acetone (3 mL). The solution was cooled to 0 °C, and Jones reagent (220 μL) was added dropwise by means of a syringe. 2-Propyl alcohol (2 mL) was added, and the reaction mixture was poured into water and extracted with Et_2O. The ether extracts were washed with saturated sodium hydrogen carbonate, dried over $MgSO_4$, and then concentrated to dryness. The resulting yellow, oily material was subjected to column chromatography (silica gel; 2/1 hexane/EtOAc) to give 76.7 mg (46% yield) of (*R*)-(+)-2-oxa-3-phenylcyclopentanone: $[\alpha]_D^{20}$ = +27.4° (*c* = 1.1, $CHCl_3$) (lit.[23] $[\alpha]_D^{23}$ = −32.5° (*c* = 4.3, $CHCl_3$) for *S* isomer); ^1H NMR ($CDCl_3$) δ 2.07–2.47 (m, 1 H), 2.52–2.78 (m, 3 H), 5.51 (dd, *J* = 7.7, 6.4 Hz, 1 H), 7.34 (m, 5 H); IR (KBr) 1776, 1176, 1142 cm^{-1}; MS (EI) *m*/*z* (relative intensity) 162 (100), 107 (87), 105 (61), 77 (35).

Determination of Absolute Configuration of (*S*)-(−)-2a. The absolute configuration of (−)-**2a** was determined to be *S* by converting it into 2-phenyltetrahydrofuran, which showed a sign of optical rotation opposite to that of (*R*)-(+)-2-phenyltetrahydrofuran derived from (*R*)-(−)-**1a**.

(a) Preparation of (*R*)-(+)-2-Phenyltetrahydrofuran. The Wilkinson catalyst $RhCl(PPh_3)_3$ (11.8 mg) was placed in a Schlenk tube equipped with a stirring bar, a rubber septum cap, and a balloon containing dihydrogen gas. Benzene (1 mL) was added at room temperature, and the resulting solution was saturated with dihydrogen by passing the gas through the solution for 10 min. (*R*)-(−)-**1a** of 93% ee (103.3 mg, 0.704 mmol) was added, and the mixture was stirred at room temperature for 1 h. GLC analysis revealed consumption of **1a**. The rhodium catalyst was removed by column chromatography (Florisil, hexane), and the eluate was concentrated to dryness to give (*R*)-(+)-2-phenyltetrahydrofuran of 90% ee as confirmed by ^1H NMR analysis using optically active Eu(hfc)$_3$ (101.7 mg, 97% yield): $[\alpha]_D^{20}$ = +45.0 (*c* = 1.1, $CHCl_3$); ^1H NMR ($CDCl_3$) δ 1.68–2.43 (m, 4 H), 3.97 (m,

(23) Manzocchi, A.; Casati, R.; Fiecchi, A.; Santaniello, E. *J. Chem. Soc., Perkin Trans. 1* **1987**, 2753.

Table V. Crystal Data and Details of the Structure Determination for $PdCl_2$\{(*R*)-BINAP\}

Crystal Data	
formula	$C_{44}H_{32}Cl_2P_2Pd$
fw	800.00
habit	prismatic
cryst syst	tetragonal
space group	$P4_1$ (No. 76)
a, Å	11.751(1)
c, Å	26.538(3)
V, Å^3	3664.2
Z	4
D_{calcd}, g cm^{-3}	1.45
$F(000)$	1624
μ(Mo Kα), cm^{-1}	7.62
cryst size, mm	0.5 × 0.2 × 0.2
Data Collection	
temp, K	298
diffractometer	Enraf-Nonius CAD4
radiation	Mo Kα (λ = 0.710 73 Å)
monochromator	graphite
scan type	$\omega/2\theta$
$\Delta\omega$, deg	0.75 + 0.35 tan θ
θ_{min}, θ_{max}, deg	1.0, 27.5
data set	h, 0–15; k, 0–15; l 0–34
no. of unique data	2489
no. of obsd data	1563 ($I \geq 2\sigma(I)$)
Refinement	
no. of refined param	442
R	0.036
R_w	0.045
S	1.551
$(\Delta/\sigma)_{av}$ in final cycle	0.03
min and max resd dens, e/Å^3	–0.24, 0.38

1 H), 4.06 (m, 1 H), 4.81 (t, J = 6.9 Hz, 1 H), 7.31 (m, 5 H); IR (KBr) 1060, 1028 cm^{-1}; HRMS (EI) calcd for $C_{10}H_{12}O$ 148.0888, found 148.0895.

(b) Hydrogenation of (–)-2a. The Wilkinson catalyst $RhCl(PPh_3)_3$ (4.1 mg) was placed in a Schlenk tube equipped with a stirring bar, a rubber septum cap, and a balloon containing dihydrogen gas. Benzene (1 mL) was added at room temperature, and the resulting solution was saturated with dihydrogen by passing the gas through the solution for 10 min. (–)-**2a** of 59% ee (33.5 mg, 0.228 mmol) was added, and the mixture was stirred at 40 °C for 2.5 h. GLC analysis revealed consumption of **2a**. The rhodium catalyst was removed by column chromatography (Florisil, hexane), and the eluate was concentrated to dryness to give (*S*)-(–)-2-phenyltetrahydrofuran of 49% ee as confirmed by ^{1}H NMR analysis using optically active Eu(hfc)$_3$ (9.2 mg, 27% yield): $[\alpha]_D^{20}$ = –17.0 (c = 0.92, $CHCl_3$).

Preparation of Pd\{(*R*)-BINAP\}$_2$. This complex appeared in the literature,[24] but little is known about its preparation and characterization. We prepared the complex by a simple method. In a Schlenk tube containing (η-allyl)(η-cyclopentadienyl)-palladium(II)[25] (84.2 mg, 0.396 mmol) and (*R*)-BINAP (500 mg, 0.803 mmol) was added benzene (5 mL) at room temperature. The system was heated at 80 °C for 3 h to give a deep red solution, which was concentrated to dryness by pumping. The resulting red solid was dissolved in dichloromethane (10 mL) and filtered through a filter-paper-tipped cannula. The filtrate was gradually concentrated under reduced pressure to ca. 4 mL, diluted with Et_2O (40 mL), and cooled to 4 °C to give reddish purple crystals of Pd\{(*R*)-BINAP\}$_2$, which was collected by filtration, washed with cold Et_2O, and dried under vacuum (480 mg, 90%). This product contained 1 equiv of Et_2O/equiv of Pd as confirmed by ^{1}H NMR spectroscopy: ^{1}H NMR (C_6D_6) δ 5.88 (t, J = 7.6 Hz, 8 H), 6.19 (t, J = 7.3 Hz, 4 H), 6.8–7.6 (m, 40 H), 7.83 (d, J = 8.2 Hz, 4 H), 8.36 (br, 8 H); ^{31}P\{^{1}H\} NMR (C_6D_6) δ 27.3. Anal. Calcd for $C_{88}H_{64}P_4Pd \cdot C_4H_{10}O$: C, 77.5; H, 5.2. Found: C, 77.0; H, 5.0.

(24) Hodgson, M.; Parker, D. *J. Organomet. Chem.* **1987**, *325*, C27. Hodgson, M.; Parker, D.; Taylor, R. J.; Ferguson, G. *Organometallics* **1988**, *7*, 1761.

(25) Tatsuno, A. G.; Yoshida, T.; Otsuka, S. *Inorg. Synth.* **1979**, *19*, 220.

Table VI. Positional and Equivalent Isotropic Thermal Parameters for $PdCl_2$\{(*R*)-BINAP\}

atom	x	y	z	B_{eq},[a] Å^2
Pd	0.47700(5)	0.02307(6)	0.500[b]	3.53(1)
Cl(1)	0.4791(3)	0.2194(3)	0.5165(2)	7.39(9)
Cl(2)	0.2808(2)	0.0199(3)	0.4830(2)	7.48(9)
P(1)	0.4990(2)	–0.1408(2)	0.45792(9)	2.89(4)
P(2)	0.6417(2)	0.0007(2)	0.54198(9)	2.93(4)
C(1)	0.6484(8)	–0.1634(7)	0.4392(4)	3.1(2)
C(2)	0.682(1)	–0.1290(9)	0.3900(4)	4.6(2)
C(3)	0.793(1)	–0.136(1)	0.3741(5)	5.7(3)
C(4)	0.880(1)	–0.167(1)	0.4093(5)	5.6(3)
C(5)	0.995(1)	–0.170(2)	0.3963(5)	8.6(5)
C(6)	1.080(1)	–0.199(2)	0.4309(6)	11.2(6)
C(7)	0.9323(8)	–0.240(1)	0.4936(5)	5.6(3)
C(9)	0.8471(8)	–0.2038(9)	0.4600(4)	3.5(2)
C(10)	0.7296(7)	–0.1979(7)	0.4737(4)	3.1(2)
C(11)	0.6602(7)	–0.1482(7)	0.5610(3)	2.8(2)
C(12)	0.6312(9)	–0.1828(9)	0.6097(4)	4.3(2)
C(13)	0.632(1)	–0.292(1)	0.6241(4)	5.8(3)
C(14)	0.671(1)	–0.3798(9)	0.5891(4)	5.1(3)
C(15)	0.667(1)	–0.494(1)	0.6044(6)	8.5(5)
C(16)	0.704(2)	–0.576(1)	0.5711(7)	9.8(5)
C(17)	0.736(1)	–0.548(1)	0.5198(8)	9.5(4)
C(18)	0.740(1)	–0.4357(9)	0.5049(6)	6.2(3)
C(19)	0.7022(9)	–0.3478(8)	0.5408(4)	4.2(2)
C(20)	0.6994(7)	–0.2293(7)	0.5258(3)	2.7(2)
C(21)	0.4546(8)	–0.2724(7)	0.4883(4)	3.7(2)
C(22)	0.3905(9)	–0.2674(9)	0.5314(4)	4.5(2)
C(23)	0.361(1)	–0.374(1)	0.5548(5)	6.6(3)
C(24)	0.395(1)	–0.475(1)	0.5351(7)	7.5(4)
C(25)	0.456(1)	–0.478(1)	0.4894(6)	6.4(3)
C(26)	0.489(1)	–0.3791(8)	0.4664(5)	4.8(3)
C(27)	0.4207(8)	–0.1311(9)	0.3992(4)	4.4(2)
C(28)	0.3614(8)	–0.218(1)	0.3353(5)	7.9(4)
C(30)	0.294(1)	–0.124(2)	0.3106(5)	11.5(5)
C(31)	0.356(1)	–0.018(2)	0.3266(6)	9.9(5)
C(32)	0.423(1)	–0.026(1)	0.3732(5)	7.8(4)
C(33)	0.7729(8)	0.0447(7)	0.5117(4)	3.6(2)
C(34)	0.8794(8)	0.0105(8)	0.5315(4)	3.9(2)
C(35)	0.9758(9)	0.0427(9)	0.5107(6)	6.0(3)
C(36)	0.976(1)	0.105(1)	0.4637(6)	7.1(4)
C(37)	0.872(1)	0.135(1)	0.4444(6)	6.9(3)
C(38)	0.769(1)	0.1083(8)	0.4678(4)	4.8(3)
C(39)	0.635(1)	0.0760(9)	0.6027(4)	4.5(2)
C(40)	0.729(1)	0.1373(9)	0.6183(4)	5.9(3)
C(41)	0.711(1)	0.202(1)	0.6650(5)	9.4(4)
C(42)	0.610(2)	0.207(2)	0.6932(7)	11.5(6)
C(43)	0.523(2)	0.142(2)	0.6711(6)	10.9(5)
C(44)	0.526(1)	0.079(1)	0.6265(5)	7.7(4)

[a] $B_{eq} = {}^4/_3\sum_i\sum_j\beta_{ij}\mathbf{a}_i\mathbf{a}_j$. [b] The z coordinate of Pd was fixed to define the origin.

X-ray Diffraction Study of $PdCl_2$\{(*R*)-BINAP\}. (a) Preparation. A solution of 249 mg (0.40 mmol) of (*R*)-BINAP in 4.0 mL of benzene was added with stirring to a mixture of 104 mg (0.40 mmol) of $PdCl_2(MeCN)_2$ in 4.0 mL of benzene, and the mixture was stirred overnight. The yellow precipitate that formed was collected by filtration, washed with benzene, and dried under vacuum. The crude product was dissolved in acetone, layered with hexane, and allowed to stand at room temperature to give red crystals of the title compound, suitable for X-ray study (238 mg, 75% yield): mp 255–260 °C dec; $[\alpha]_D^{20}$ = +682° (c = 0.5, $CHCl_3$). Anal. Calcd for $C_{44}H_{32}Cl_2P_2Pd$: C, 66.06; H, 4.03; Cl, 8.86; P, 7.74. Found: C, 65.82; H, 3.93; Cl, 8.96; P, 7.77.

(b) Determination and Refinement of the Structure. A single crystal of dimensions ca. 0.5 × 0.2 × 0.2 mm was sealed in a glass capillary tube under argon. Intensity data were collected on a Enraf-Nonius CAD4 four-circle diffractometer. Unit cell dimensions were obtained from a least-squares treatment of the setting angles of 25 reflections in the range 11 < θ < 14°. The cell dimensions suggested a tetragonal cell, and systematic absences in the diffractometer data indicated the space group $P4_1$. Diffraction data were collected in the range 1.0 < θ < 27.5° using the $\omega/2\theta$ scan technique. The scan rate varied from 1 to 10°/min in ω. Three standard reflections, monitored every 60 h of X-ray exposure, showed no significant variation in the intensities during the data collection. The data were corrected

for absorption and for Lorentz and polarization effects. Of the 2489 unique reflections measured, 1563 were classified as observed ($I > 2\sigma(I)$), and these were used for the solution and refinement of the structure.

Calculations were performed on a DEC MicroVAXII computer using the SDP package (version 3.0) provided by Enraf-Nonius. The scattering factors were taken from ref 26. The palladium atom was located from a Patterson map (MITHRIL), and the other non-hydrogen atoms were found from subsequent difference Fourier syntheses. Hydrogen atoms were not located. The structure was refined by full-matrix least squares with anisotropic thermal parameters for all non-hydrogen atoms. The function minimized in least squares was $\Sigma w(|F_o|-|F_c|)^2$ ($w = 4I/[\sigma^2(I) + (0.05I)^2]$). The final R index was 0.036 ($R_w = 0.045$, $S = 1.55$). $R = \Sigma||F_o| - |F_c||/\Sigma|F_o|$, $R_w = [\Sigma w(|F_o| - |F_c|)^2/\Sigma w|F_o|^2]^{1/2}$, and $S = [\Sigma w(|F_o|-|F_c|)^2/(N_o-N_p)]^{1/2}$, where N_o is the number of observed data and N_p is the number of parameters varied. The crystal data and details of data collection and refinement are summarized in Table V. The positional and equivalent thermal parameters are listed in Table VI.

(26) Cromer, D. T.; Waber, J. T. *International Tables for X-ray Crystallography*; Kynoch Press: Birmingham, U. K., 1974; Vol, IV, Table 2.2B.

Acknowledgment. This work was supported by a Grant-in-Aid for Scientific Research from the Ministry of Education, Science and Culture of Japan and by Asahi Glass Foundation.

Supplementary Material Available: Listings of all bond distances and angles and anisotropic thermal parameters (5 pages). Ordering information is given on any current masthead page.

OM930365A